Free Radical Biology and Medicine 97 (2016) 124–135

Contents lists available at ScienceDirect

Free Radical Biology and Medicine

journal homepage: www.elsevier.com/locate/freeradbiomed

Detailed protocol to assess *in vivo* and *ex vivo* myeloperoxidase activity in mouse models of vascular inflammation and disease using hydroethidine ☆

Jihan Talib [a], Ghassan J. Maghzal [a], David Cheng [a], Roland Stocker [a,b,*]

[a] Vascular Biology Division, Victor Chang Cardiac Research Institute, Darlinghurst, New South Wales 2010, Australia
[b] School of Medical Sciences, University of New South Wales, Sydney, Australia

ARTICLE INFO

Article history:
Received 5 November 2015
Received in revised form
30 April 2016
Accepted 6 May 2016
Available online 13 May 2016

Keywords:
3-Chlorotyrosine
Myeloperoxidase
Mass spectrometry
Hypochlorous acid
Hydroethidine
Arteries
Inflammation
Atherosclerosis
Biomarker

ABSTRACT

Myeloperoxidase (MPO) activity contributes to arterial inflammation, vascular dysfunction and disease, including atherosclerosis. Current assessment of MPO activity in biological systems *in vivo* utilizes 3-chlorotyrosine (3-Cl-Tyr) as a biomarker of hypochlorous acid (HOCl) and other chlorinating species. However, 3-Cl-Tyr is formed in low yield and is subject to further metabolism. Recently, we reported a method to selectively assess MPO-activity *in vivo* by measuring the conversion of hydroethidine to 2-chloroethidium (2-Cl-E^+) by liquid chromatography with tandem mass spectrometry (LC–MS/MS) (J. Biol. Chem., 289, 2014, pp. 5580–5595). The hydroethidine-based method has greater sensitivity for MPO activity than measurement of 3-Cl-Tyr. The current methods paper provides a detailed protocol to determine *in vivo* and *ex vivo* MPO activity in arteries from mouse models of vascular inflammation and disease by utilizing the conversion of hydroethidine to 2-Cl-E^+. Procedures for the synthesis of standards, preparation of tissue homogenates and the generation of 2-Cl-E^+ are also provided in detail, as are the conditions for LC–MS/MS detection of 2-Cl-E^+.

1. Introduction

Myeloperoxidase (MPO) is a heme-containing enzyme proposed to provide an important mechanistic link between inflammation, oxidation and related diseases, particularly cardiovascular diseases (for reviews see [1,2]). In the presence of hydrogen peroxide (H_2O_2), MPO oxidizes chloride (Cl^-) to the highly reactive hypochlorous acid (HOCl) [3,4]. MPO/HOCl contribute to oxidative stress within and affect the function of arteries via multiple mechanisms, including uncoupling of endothelial nitric oxide synthase and the oxidation of apolipoproteins [5–7]. For example, in a hospital-based population, the serum concentration of MPO is a strong and independent predictor of endothelial dysfunction [8], whereas in patients with major adverse cardiac events, elevated serum/plasma concentrations of MPO have been shown to predict the patient's 6-month outcome [9,10].

The adverse effects of MPO activity in cardiovascular disease have been attributed primarily to its role in the pathogenesis of atherosclerosis [11,12], the basis of most cardiovascular diseases and the leading cause of morbidity and mortality in the developed world [13]. Atherosclerosis is a multi-factorial disease of arteries characterized by a state of endothelial dysfunction, accumulation of cholesterol, heightened oxidative stress and inflammation in the arterial wall, including the deposition of enzymatically active MPO by infiltrating phagocytes [14]. Indeed, HOCl-modified low (LDL) and high-density lipoproteins (HDL) have been detected in human atherosclerotic lesions using a monoclonal antibody raised against HOCl-modified LDL [15], and by measuring 3-chlorotyrosine (3-Cl-Tyr) by stable isotope dilution gas chromatography-mass spectrometry, respectively [16,17].

Abbreviations: *Apoe*$^{-/-}$, apolipoprotein E gene knockout; CE, collision energy; 2-Cl-E^+, 2-chloroethidium; 2-Cl-E^+- d_5, deuterated 2-chloroethidium; 3-Cl-Tyr, 3-chlorotyrosine; DTPA, diethylene triamine pentaacetic acid; E^+-E^+, diethidium; E^+, ethidium; HOCl, hypochlorous acid; HE, hydroethidine; HE-d_5, deuterated hydroethidine; 2-OH-E^+, 2-hydroxyethidium; MPO, myeloperoxidase; *Mpo*$^{-/-}$, myeloperoxidase gene knockout; MRM, multiple reaction monitoring

☆Funding: This work was supported by the Australian Research Council Discovery Project 110102135 and by the National Health and Medical Research Council of Australia Project Grants 1020776 and 1080604. RS acknowledges support from Senior Principal Research Fellowships 1003484 and 1111632 from the National Health and Medical Research Council of Australia.

* Corresponding author at: Vascular Biology Division, Victor Chang Cardiac Research Institute, Lowy Packer Building, 405 Liverpool Road, Darlinghurst NSW 2010, Australia.
E-mail address: r.stocker@victorchang.edu.au (R. Stocker).

http://dx.doi.org/10.1016/j.freeradbiomed.2016.05.004
0891-5849/

The ability to measure MPO activity in mouse arterial tissue is important for several reasons. Foremost, it is required to progress our current understanding of the roles of MPO in vascular pathologies including atherosclerosis, given that such diseases are studied commonly in mouse models. Just as importantly, it is essential to validate target engagement of MPO inhibitors including the recently developed thioxanthines [18,19] that are promising tools to assess the extent of contribution of MPO activity to arterial and other diseases. To date, detection of *in vivo* MPO catalytic activity within arterial tissue from mouse models of vascular disease and atherosclerosis has been limited. This is likely due to the insensitivity of existing assays to measure MPO activity, combined with the fact that the MPO content in murine phagocytes is only about 10–20% of the human counterparts [20]. Indeed, ascertaining a direct role of MPO in atherogenesis using mouse models has yielded conflicting results, with both MPO deficiency [21] and overexpression [22] increasing atherosclerotic lesion size. Importantly, all of the previous studies assessing the role of MPO in murine atherosclerosis [21–24] were unable to detect 3-Cl-Tyr or did not measure MPO activity in arterial tissue. This lead to the conclusion that macrophages in mouse atherosclerotic tissue do not express MPO, and that mice are an inappropriate model for testing the role of MPO in vascular disease [22].

Currently, 3-Cl-Tyr is considered to be the gold standard biomarker for assessing MPO activity [25]. However, the low reaction rate of HOCl with tyrosine residues ($\sim 40\ M^{-1}\ s^{-1}$) [26] and the possible further metabolism of 3-Cl-Tyr in biological systems [27,28] present serious limitations in the utility of 3-Cl-Tyr as a biomarker for MPO activity. Other methods reported for the assessment of MPO activity *in vivo* include the fluorescent probe Amplex Red® [29–32] and the chemiluminescent probe L-012 [33]. Both assays require capture of MPO from a biological system followed by the detection of oxidized products of Amplex Red® or L-012-derived luminescence. However, both probes lack specificity to MPO/HOCl. Thus, Amplex Red® is oxidized readily by peroxidases other than MPO including proteins with peroxidase activity such as cytochrome *c* [34], while L-012 also emits luminescence in the presence of peroxidase/H_2O_2 [35]. Other potential biomarkers of MPO/HOCl include chlorinated plasmalogens and glutathione sulfonamide [25]. Of these, chlorinated lipids such as 2-chlorohexadecanal detected by gas chromatography mass spectrometry have been reported to be elevated in human atherosclerotic lesions [36], although we are unaware of reports on the presence of chlorofatty aldehydes or glutathione sulfonamide in arteries of mouse models of vascular disease including atherosclerosis. Although MPO-mediated oxidation of taurine [18], urate [18], monochlorodimedone [5,37] and 4-hydroxyphenylacetic acid [37] have been used successfully to assess MPO activity *in vitro* and *ex vivo*, there has been no evidence for the utility of these methods to determine *in vivo* MPO activity in mouse arterial tissue. In light of these limitations there is an ongoing quest to develop specific and sensitive methods to assess MPO-activity in arterial tissue *in vivo*, particularly in the context of murine models of vascular diseases.

We reported recently that MPO activity can be assessed *in vivo* and *in vitro* by the conversion of hydroethidine (HE) to 2-chloroethidum (2-Cl-E^+), and that 2-Cl-E^+ is a superior biomarker than 3-Cl-Tyr in mouse models of peritonitis and arterial inflammation [38]. This was the first report on the utilization of an exogenous probe to assess *in vivo* MPO activity in mouse arterial tissue. Hydroethidine has been used for over 25 years as a probe to measure superoxide radical anion ($O_2^{\cdot -}$) in biological systems [39]. Initially, $O_2^{\cdot -}$ was thought to oxidize HE to the red fluorescent product ethidium (E^+), until Kalyanaraman and co-workers identified 2-hydroxyethidum (2-OH-E^+) as the specific product of HE oxidation by $O_2^{\cdot -}$ [40]. Other oxidants including H_2O_2 and ferricytochrome *c* convert HE to E^+ and E^+-E^+ dimers [41,42]. We showed that 2-Cl-E^+ is the specific product of HE oxidation by the MPO-derived oxidants HOCl and chloramines [38]. Using this method, we also demonstrated the utility of HE as a multi-purpose probe to simultaneously determine HOCl/chlorinating activity as well as $O_2^{\cdot -}$, using liquid chromatography/tandem mass spectrometry (LC–MS/MS) and in-house synthesized deuterated internal standards [38].

The procedures listed herein details methods to use 2-Cl-E^+ for the assessment of *in vivo* and *ex vivo* MPO activity from arterial tissue of mouse models of vascular disease. The mouse models referred to in this methods paper include a model of vascular inflammation [38,43] and a model of vulnerable atherosclerotic plaque [44]. HE is the first multi-purpose probe that can be used to detect *in vivo* MPO activity in mouse arterial tissue and therefore can be used to potentially elucidate the role of MPO in pathological events that contribute to the development of vascular diseases including atherosclerosis.

2. Principles

It was first reported 20 years ago that HE reacts with HOCl to form a product with fluorescence characteristic similar to that of E^+ [45]. We established that this product in fact is 2-Cl-E^+ and proposed that direct electrophilic attack on the *ortho*-C2 position of HE by HOCl and chloramines forms 2-Cl-E^+ specifically (Scheme 1) [38]. Oxidation of HE by H_2O_2, $O_2^{\cdot -}$, hydroxyl radical, *t*-butyl hydroperoxide, *t*-butyl peroxyl radical, peroxynitrite or via a radical mechanism did not lead to the conversion of HE to 2-Cl-E^+ [38].

2.1. Advantages of 2-Cl-E^+ over 3-Cl-Tyr to determine MPO activity in mouse arterial tissue

As reviewed recently [25] and described briefly above, there are several probes that principally can be used to assess MPO/HOCl activity. We limited our comparison to 3-Cl-Tyr, as this biomarker is regarded the gold standard for detection of *in vivo* MPO activity.

Compared with 3-Cl-Tyr, there are several advantages to using 2-Cl-E^+ to assess MPO activity. The rate of reaction of HE with HOCl, estimated using competition kinetics with urate ($1.5 \times 10^5\ M^{-1}\ s^{-1}$) [38], is four orders of magnitude faster than that for the reaction of HOCl with tyrosine ($\sim 40\ M^{-1}\ s^{-1}$), indicating that HE is a much more sensitive probe for HOCl than tyrosine. The amounts of 3-Cl-Tyr detected are dependent on tissue concentration of tyrosine, the extent of 3-Cl-Tyr oxidation to 3,5-dichlorotyrosine, mono- and dicholorinated 4-hydroxyphenylacetylaldehyde [46,47], and the de-chlorination and metabolism of 3-Cl-Tyr [28]. As a result, measuring steady-state concentrations of tissue 3-Cl-Tyr is unlikely to accurately reflect the amount of active MPO present. In contrast, HE concentration can be manipulated to ensure comparable substrate concentrations in different biological samples and to suitably compete against alternate HOCl substrates. Furthermore, the application of HE to arterial tissue allows for detection of “ongoing” chlorination activity, and hence can be determined at different stages of chronic arterial inflammation and atherosclerotic plaque formation. By comparison, 3-Cl-Tyr does not represent ongoing chlorinating activity. Rather, it reflects a steady-state situation that is determined by the rate of *in situ* formation and removal of 3-Cl-Tyr.

We compared tissue concentrations of 3-Cl-Tyr versus 2-Cl-E^+ in an *in vivo* model of arterial inflammation and an *in vivo* model of vulnerable atherosclerotic plaque. In the first model, a non-occlusive cuff is placed around the left femoral artery. The placement of the cuff causes acute and then sustained localized inflammation

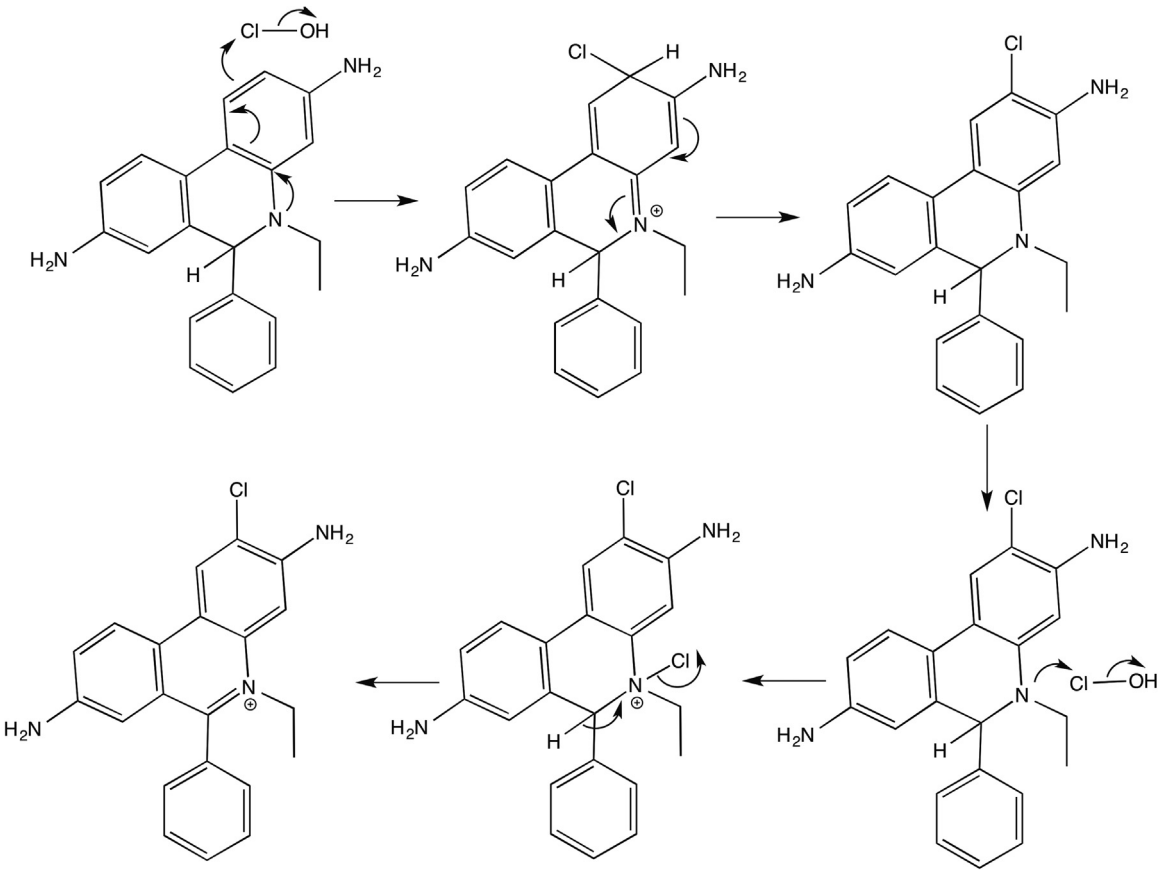

Scheme 1. Proposed mechanism for the formation of 2-Cl-E$^+$ from the reaction of HOCl with HE. Reproduced from Ref. [38] with permission.

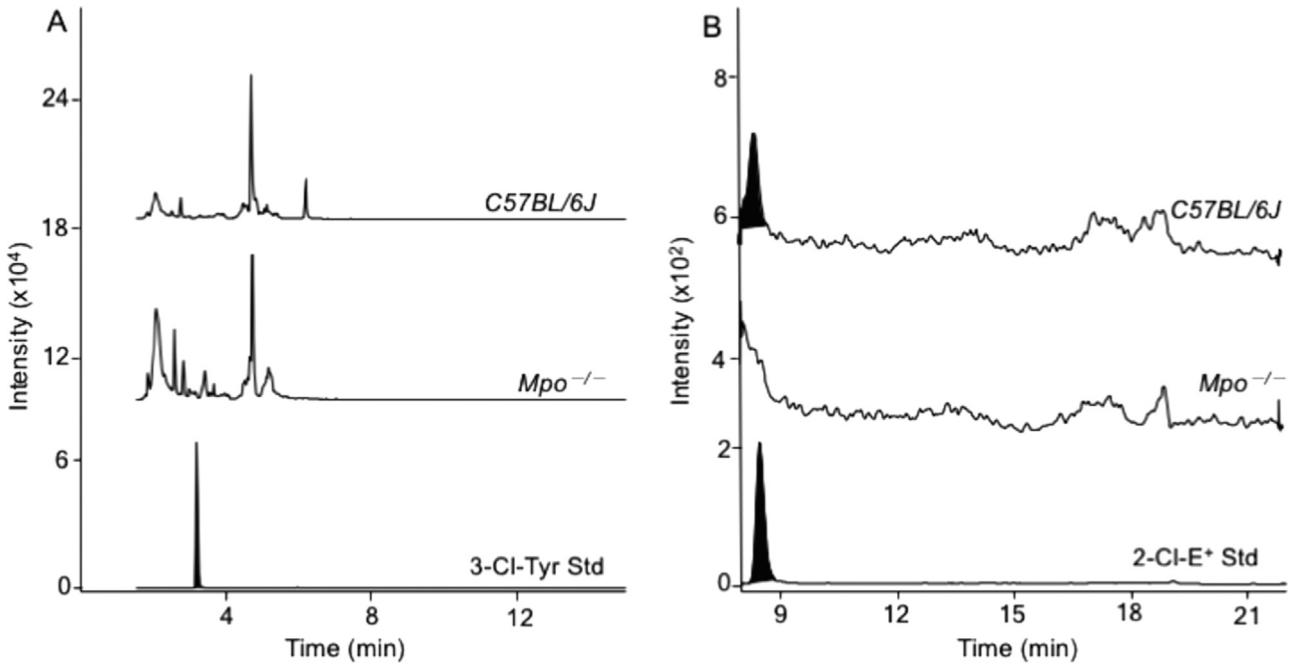

Fig. 1. *In vivo* detection of 2-Cl-E$^+$ but not 3-Cl-Tyr in mouse arteries. (A) Absence of 3-Cl-Tyr and (B) detection of 2-Cl-E$^+$ in the "cuffed" left femoral artery of a C57BL/6J mouse model of inflammation. 3-Cl-Tyr and 2-Cl-E$^+$ were both absent in "cuffed" left femoral artery of *Mpo*$^{-/-}$ mice (not shown). Mice (8–9 weeks) were fed chow for 1 week prior to the placement of a non-occlusive cuff around the left femoral artery to induce arterial inflammation for 14 days. HE (80 μL of 20 mM) was administered by intravenous injection 60 min prior to collection of the femoral artery, as described previously [38].

characterized by infiltration of polymorphonuclear leukocytes [43,48,49]. Despite this strong neutrophil response, 3-Cl-Tyr could not be detected in cuffed arteries of wild type and *Mpo*$^{-/-}$ mice (Fig. 1A). In contrast, cuff placement followed by intravenous injection of HE yielded 2-Cl-E$^+$ detected by LC–MS/MS analysis of isolated cuffed arteries of wild type C57BL/6J mice (Fig. 1B).

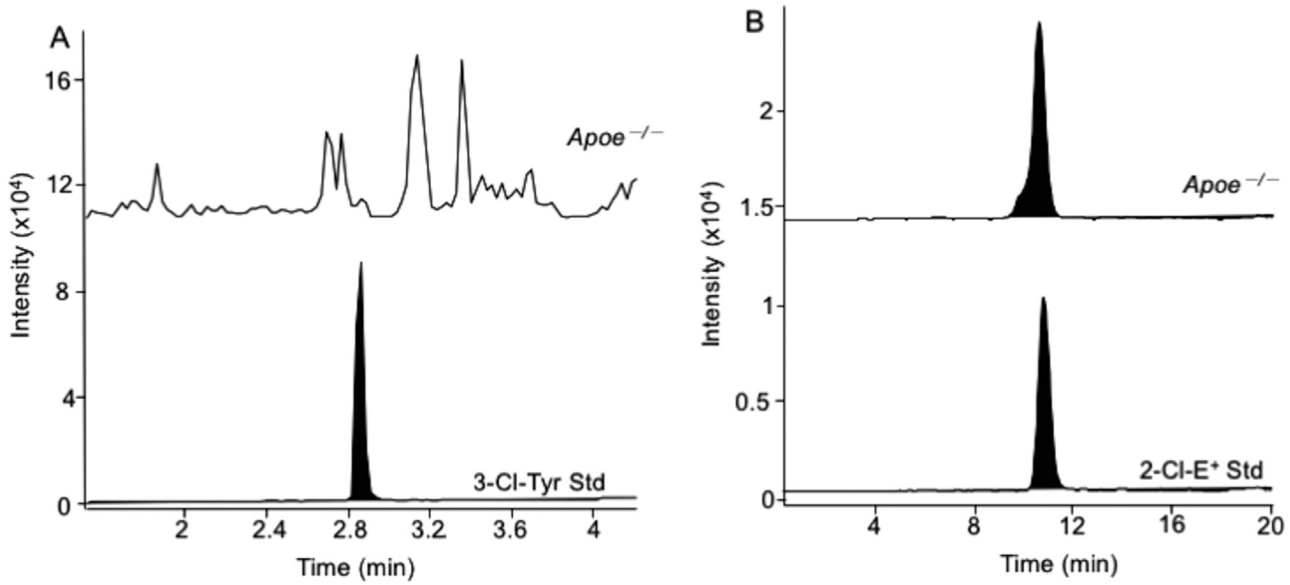

Fig. 2. (A) Absence of 3-Cl-Tyr and (B) detection of 2-Cl-E$^+$ in stable plaques of the right carotid artery from the mouse model of vulnerable atherosclerotic plaque. Vulnerable atherosclerotic plaques were induced in the right carotid artery by tandem stenosis in male *Apoe*$^{-/-}$ mice fed a Western diet for 6 weeks. Following placement of the two ligations, mice were fed Western diet for another 7 weeks [44], before HE (80 μL of 20 mM) was administered by intravenous injection and arteries collected 45 min after HE injection. *Note:* Retention times for 3-Cl-Tyr and 2-Cl-E$^+$ can vary over time and/or between analyses.

Importantly, 2-Cl-E$^+$ was not detected in the cuffed artery of *Mpo*$^{-/-}$ mice (Fig. 1B), providing strong evidence for arterial 2-Cl-E$^+$ being formed specifically by local MPO activity.

Similar observations were made using the murine model of vulnerable atherosclerotic plaque (Fig. 2). In this model, two ligations (150 μm in diameter) are introduced 3 mm apart to the right carotid artery of apolipoprotein E-deficient (*Apoe*$^{-/-}$) mice fed a Western diet [44]. These ligatures changes the blood flow such that unstable and stable atherosclerotic plaques are formed proximate and distal to second ligature, respectively, of the right carotid artery [44]. These unstable plaques did not contain measurable amounts of 3-Cl-Tyr (Fig. 2A). In contrast, intravenous administration of HE 45 min prior to tissue collection resulted in detection of 2-Cl-E$^+$ in both unstable and stable atherosclerotic lesions of the right carotid artery (Fig. 2B). Thus, in these models of vascular inflammation and atherosclerosis, *in vivo* conversion of HE to 2-Cl-E$^+$ was able to detect arterial MPO activity under conditions where 3-Cl-Tyr could not be detected.

2.2. Limitations of using 2-Cl-E$^+$ as a biomarker to assess MPO activity

Like for every biomarker, there are limitations to using 2-Cl-E$^+$ to assess *in vivo* MPO activity. First, the amounts of 2-Cl-E$^+$ detected in a tissue do not directly equate to the amounts of HOCl generated owing to competition with other HOCl scavengers and, possibly, the conversion of HE to oxidation products other than 2-Cl-E$^+$. Similarly, the absence of 2-Cl-E$^+$ cannot be interpreted unambiguously as an absence of active MPO, as it may result from too little MPO to effectively compete for HE. Secondly, detection of 2-Cl-E$^+$ requires a chromatographic separation of the HE oxidation product, ideally coupled to mass spectrometry. Fluorescence is not suitable to detect 2-Cl-E$^+$, because 2-Cl-E$^+$ is only weakly fluorescent and its fluorescence spectrum overlaps with that of E$^+$ and 2-OH-E$^+$ [38]. Despite this, the *in vivo* procedure described herein can detect $\geq$100 attomol 2-Cl-E$^+$ within as little as $\sim$0.2 mg arterial tissue.

Similar to other probes (*vide supra*), HE can also be used to determine MPO-activity in mouse tissue *ex vivo*. Such *ex vivo* application shows a high degree of sensitivity as both, hydrogen peroxide (H_2O_2) required for the activation of endogenous MPO, and the substrate (HE) can be manipulated readily to promote formation 2-Cl-E$^+$. While this approach assesses the amount of MPO present in the tissue, it does not reflect endogenous MPO activity. Furthermore, the *ex vivo* MPO activity determined could conceivably be affected by tissue extraction and homogenization. Lastly, we cannot exclude the possibility that 2-Cl-E$^+$ is subject to dechlorination *in vivo*. However, despite these limitations, the amount of 2-Cl-E$^+$ generated in arterial tissue by *in vivo* or *ex vivo* detection under different conditions can be compared and semi-quantitative data on MPO activity can be obtained.

Here we provide in detail the procedures for the *in vivo* and *ex vivo* assessment of MPO activity in arterial tissue from mouse models of vascular inflammation and vulnerable atherosclerotic plaque (outlined in Fig. 3). The procedure for *in vivo* assessment of MPO activity follows our original publication [38], including the synthesis of deuterated HE (HE-d_5) required for preparation of the internal standard, 2-Cl-E$^+$-d_5, and details on the retro-orbital injection of HE in mice. The procedure for the determination of *ex vivo* MPO activity describes tissue homogenization, treatment of the homogenate with glucose/glucose oxidase to generate H_2O_2, and HE addition to the homogenate. Finally, the steps required for LC–MS/MS determination of 2-Cl-E$^+$ in the arterial homogenates are listed.

3. Preparation of HE-d_5

HE-d_5 can be custom-synthesized, *e.g.*, by Chemaphor Chemical Services of Avivagen Inc. (Ottawa, Canada), or prepared in-house as described below.

3.1. Synthesis of ethidium iodide-d_5-diethyl carbamate

Ethidium iodide-d_5-diethyl carbamate is synthesized by reacting diethyl (6-phenyl-10,10*a*-dihydrophenanthridine-3,8-diyl)dicarbamate with nitromethane, iodoethane-d_5 [38,50].

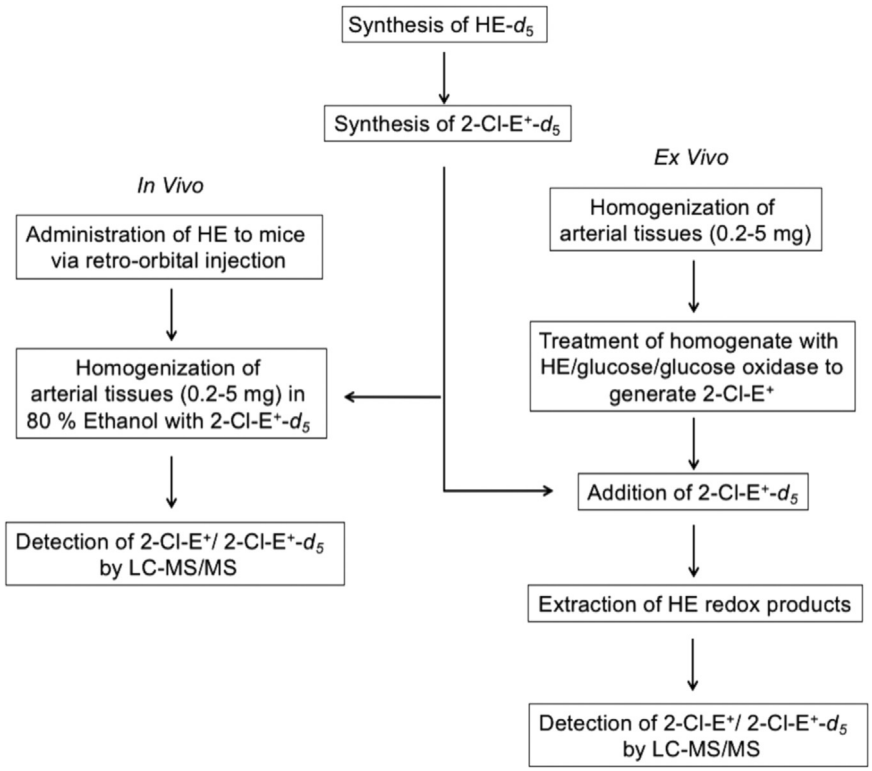

Fig. 3. Outline of the procedures used for LC–MS/MS detection of *in vivo* and *ex vivo* 2-Cl-E$^+$ in mouse arteries.

3.1.1. Materials

- Diethyl (6-phenyl-10,10*a*-dihydrophenanthridine-3,8-diyl)dicarbamate, synthesized from 3,8-diamino-6-phenylphenanthridine (Sigma-Aldrich, 338966) as described previously [50]
- Nitromethane
- Iodoethane-d_5 (Sigma-Aldrich, 324582)
- Dichloromethane (Sigma-Aldrich, 650463)

3.1.2. Equipment

- Magnetic hotplate with temperature control
- Rotavapor® (Büchi, RE111)
- Sintered Büchner funnel with ST joint (Sigma-Aldrich, Z546895)
- Erlenmeyer flask with ST joint (Sigma-Aldrich, Z723088)
- Evaporating flask, pear-shaped (Sigma-Aldrich, Z515531)

3.1.3. Protocol

1. To 415 mg diethyl (6-phenyl-10,10*a*-dihydrophenanthridine-3,8-diyl)dicarbamate in nitromethane add 0.78 mL iodoethane-d_5 under constant stirring.
2. Heat the reaction mixture to 100 °C and leave for 7 days under constant stirring.
3. Allow the reaction mixture to cool to room temperature and collect the bright yellow precipitate via vacuum filtration using a sintered Büchner funnel and Erlenmeyer flask.
4. Wash the bright yellow precipitate with dichloromethane (3 × 20 mL) and transfer to a pear-shaped evaporating flask and dry product *in vacuo via* rotary evaporation.

3.2. Synthesis of ethidium bromide-d_5 [38,51]

3.2.1. Materials

- Ethidium iodide-d_5-diethyl carbamate (see procedure above)
- 48% w/v Hydrobromic acid (Ajax Australia, 254–500 mL)
- 28% Ammonium hydroxide (Sigma-Aldrich, 221228)
- Dichloromethane (Sigma-Aldrich, 650463)
- Magnesium sulfate (Sigma-Aldrich, 63136)

3.2.2. Equipment

- Liebig condenser (Sigma-Aldrich, Z530964)
- Round bottom flask (Sigma-Aldrich, CLS4320C50)
- Quickfit® separating funnel (Sigma-Aldrich, Z304263)
- Rotavapor® (Büchi, RE111)
- Evaporating flask, pear-shaped (Sigma-Aldrich, Z402982)
- Column for flash chromatography (Sigma-Aldrich, Z147478)
- 230–400 mesh silica gel (Scharlau, Spain)

3.2.3. Protocol

1. Reflux ethidium iodide-d_5-diethyl carbamate (300 mg) in 48% w/v hydrobromic acid (1 mL) overnight.
2. Cool reaction mixture to room temperature and basify with 38% w/v ammonium hydroxide solution.
3. Extract with 3 × 100 mL dichloromethane and dry combined organic extracts with magnesium sulfate.
4. Transfer organic extract to an evaporating flask and evaporate using Rotavapor®.
5. Purify the resultant dark-brown residue by flash chromatography over silica gel using a gradient of 0:100–20:80 (methanol/dichloromethane).
6. Combine collected fractions and evaporate to give ethidium bromide-d_5 as a bright orange solid.

3.3. Synthesis of hydroethidine-d_5 [52]

3.3.1. Materials

- Ethidium bromide-d_5

- Methanol (Merck, 1.06009)
- Sodium borohydride (Ajax Australia)
- Dichloromethane (Sigma-Aldrich, 650463)
- Magnesium sulfate (Sigma-Aldrich, 63136)
- 230–400 Mesh silica gel (Scharlau, Spain)

3.3.2. Equipment

- Magnetic hotplate with temperature control
- Rotavapor® (Büchi, RE111)
- Evaporating flask, pear-shaped (Sigma-Aldrich, Z515604)
- Quickfit® separating funnel (Sigma-Aldrich, Z304263)
- Column for flash chromatography (Sigma-Aldrich, Z147478)

3.3.3. Protocol

1. Add 80 mg ethidium bromide-d_5 and 20 mg sodium borohydride to 5 mL methanol under constant stirring. Allow the reaction mixture to stir for 10 min at room temperature. The reaction mixture will change from orange to colorless.
2. Remove the solvent via rotary evaporation and re-dissolve the resulting precipitate in 50 mL dichloromethane.
3. Wash dichlormethane with 3×50 mL water.
4. Dry the organic layer (dichloromethane) with magnesium sulfate and evaporate.
5. Purify the resulting residue by flash chromatography over silica gel using a gradient of 20:80 to 60:40 (methanol/dichloromethane) to give hydroethidine-d_5 as a purple solid.

4. Synthesis of 2-chloroethidium and 2-chloroethidium-d_5

4.1. Materials

- 1 mM HE or HE-d_5. First, prepare 15 mM HE from the commercial stock by adding 211 µL argon-flushed DMSO to 1 mg HE (Tyger Scientific, H12500) under dim lighting and away from fluorescent and artificial light. The concentration of HE should be confirmed via spectrophotometry using $\varepsilon_{265\ nm} = 1.8 \times 10^4\ M^{-1}\ cm^{-1}$ and $\varepsilon_{345\ nm} = 9.75 \times 10^3\ M^{-1}\ cm^{-1}$ [53]. Briefly, add 2.5 µL of 15 mM HE in DMSO to 997.5 µL PBS (containing 0.05 mM DTPA) in a quartz cuvette, mix by inversion and obtain the UV–visible spectrum in the 200–600 nm range. Subtract the spectrum of the corresponding blank (DMSO only) and calculate the HE concentration from the absorbance values at 345 and 265 nm. Aliquots of 15 mM HE can be stored in argon-flushed microcentrifuge tubes and stored at −80 °C for up to 2 months. Under dim lighting, dilute 15 mM HE to 1 mM in ethanol pre-flushed with N_2.
- Dimethyl sulfoxide (DMSO) (Sigma-Aldrich, 276855)
- Phosphate buffer saline (PBS)
- Bleach (TrueBlue Chemicals, 40 g/L NaOCl)
- 200 mM Potassium hydroxide (KOH, Sigma-Aldrich, P5958)
- 20 mM Trolox® (5 mg of Trolox®, Sigma-Aldrich; 238813) in 1 mL ethanol pre-flushed with N_2
- Ethanol (Sigma-Aldrich, 459858) flushed with N_2

4.2. Equipment

- Spectrophotometer (Agilent, Cary 100 UV–vis), equipped with quartz cuvettes (PerkinElmer, B0631118)

4.3. Protocols

4.3.1. Determination of HOCl concentration

1. Dilute bleach 1/100 in nanopure water.
2. Set spectrophotometer to 292 nm and blank the absorbance using 200 mM KOH in the quartz cuvette.
3. Add 200 µL of bleach to 800 µL of 200 mM KOH in a quartz cuvette and measure absorbance at 292 nm.
4. Calculate the HOCl concentration using the Beer-Lambert law and $\varepsilon_{292\ nm} = 350\ M^{-1}\ cm^{-1}$.

4.3.2. Preparation and extraction of 2-Cl-E^+ or 2-Cl-E^+-d_5

1. Under dimed light, add the reagents listed below in the order listed in a 1.7 mL micro-centrifuge tube.
   - 175 µL PBS
   - 25 µL 20 mM Trolox®
   - 50 µL 1 mM HE or HE-d_5
   - 250 µL 1 mM HOCl
2. Vortex and incubate the reaction mixture at room temperature for 60 min in the dark.
3. Extract 2-Cl-E^+ or 2-Cl-E^+-d_5 by diluting mixture 1/5 in ethanol pre-flushed with N_2 and leave on ice in the dark for 15 min.
4. Centrifuge samples at 17,000*g* for 20 min at 4 °C and collect supernate.
5. Isolation of 2-Cl-E^+ or 2-Cl-E^+-d_5 is achieved via semi-preparative HPLC using the conditions listed in Table 1. The fraction collected should be analyzed by mass spectrometry to confirm the identity of the isolated product. Following isolation the fractions can be freeze-dried to obtain a solid product.

5. *In vivo* detection of 2-Cl-E^+ in arterial tissue

5.1. Retro-orbital injection of HE in mice

5.1.1. Materials

- HE Working Solution. 1 mg HE (Tyger H12500) dissolved in 80 µL argon-bubbled DMSO
- Sterile saline
- Isofluorane

5.1.2. Equipment

- A microtube centrifuge (Thermo Scientific Heraeus Fresco 17 centrifuge)
- Aluminum foil
- Insulin syringe
- Anesthetic circuit
- Nose-cone T piece

5.1.3. Protocol

1. Add 40 µL HE Working Solution drop-by-drop to 35 µL sterile saline. Centrifuge at $16{,}000 \times g$ for 1 min, remove any particulates, then wrap tube with aluminium foil to protect from light.
2. Transfer solution to insulin syringe and prepare mouse for retro-orbital injection (Steps 3 – 8 below).
3. Place mouse to be injected into the induction chamber of the anesthetic machine, making sure oxygen is turned on and isoflurane is set to 4%.
4. When anesthetized, connect mouse to the anesthetic circuit via a nose cone, to allow continuous anesthesia during this

Table 1
HPLC parameters for the isolation of 2-Cl-E$^+$.

Instrument	HPLC equipped with a fraction collector		
Mobile phase A	0.1% Formic acid in water		
Mobile phase B	0.1% Formic acid/90% acetonitrile		
Column	Vydac C18 Reverse-phase, 10 μm, 250 × 10 mm		
Gradient	Time (min)	A (%)	B (%)
	0	75	25
	45	65	35
	47	0	100
	52	0	100
	55	75	25
	65	75	25
Flow rate	4 mL/min		
Detector settings	UV–vis absorption detector set at 254 nm		
Typical injection vol.	1 mL		
Retention time for 2-Cl-E$^+$	~23 min		

procedure, and lower isoflurane to 2%.
5. Ensure the mouse is on its side with the eye to be injected facing up. For right-handed operator, injection is best into the right retro-orbital sinus of the mouse. The mouse is placed in left lateral recumbency with its head facing to the right.
6. Place gentle pressure on the fur on either side of the eye. This causes the eye to bulge slightly. When retracting the skin special care must be taken not to apply pressure on the trachea and cut off the animal's air supply.
7. Insert the needle bevel down into the medial canthus (corner) of the eye at a 45° angle to the nose through the conjunctiva membrane into the vessels behind the eyeball [54]. There is a degree of resistance, which causes the eye to retreat slightly back into the sinus, until the needle pierces through the conjunctiva.
8. Gently inject 75 μL of the solution prepared in Step 1 slowly and smoothly into the retro-orbital vessel, keeping hand steady. Remove needle gently to prevent injury to the eye.
9. Keep mouse in the dark after injection. During the recovery monitor the mouse and examine the injection site for swelling or other visible trauma. If no adverse effects are observed, return the mouse to its home cage after it has regained its reflexes. If major swelling, uncontrolled bleeding or eye trauma occurs at the injection site or is observed in the mouse, euthanize the mouse immediately.
10. 45 min after injection, anesthetize mouse using isofluorane.
11. When fully anesthetized, connect the mouse to an anaesthetic circuit via a nose cone T- piece, to allow continuous anesthesia with isoflurane at 2%.

5.2. Perfusion of animal and collection of tissue

5.2.1. Materials

- Syringes (1 mL)
- Heparin tubes for collection of <1 mL blood
- 25G Needles
- PBS

5.2.2. Protocol

1. While mouse is anesthetized and connected to the anesthetic circuit, open chest and abdominal cavities, puncture left ventricle and collect ≥ 200 μL blood into heparin tubes.
2. Immediately after removal of blood, insert 25G needle into the left ventricle (same spot from where blood was collected). The needle needs to be connected to PBS-containing reservoir positioned 90 cm above the laboratory bench where mouse is placed. Note: the pressure produced by positioning the PBS reservoir 90 cm above the lab bench corresponds to physiological pressure.
3. Perfuse mouse with PBS until liver and kidneys change to a paler color.
4. Following systemic perfusion, collect required tissue and snap freeze in liquid N_2 as soon as possible. Store samples at -80 °C until analysis.

5.3. Tissue homogenization and preparation of samples and standards

5.3.1. Materials

80% Ethanol (pre-flushed with nitrogen) containing 0.4 nM 2-Cl-E$^+$-d_5.

5.3.2. Equipment

- 0.2 mL Micro tissue grinder (Wheaton; 357848)
- A microtube centrifuge (Thermo Scientific Heraeus Fresco 17 centrifuge)
- 250 μL Glass inserts with polymer feet (Agilent, 5181-1270)
- PTFE/red silicone septa (Agilent, 5182-0731)
- Amber 2 mL screw top HPLC vials (Agilent, 5188-0716)
- Screw top lid for HPLC vials (Agilent, 5182-0728)

5.3.3. Protocols

5.3.3.1. Homogenization of arterial tissue

1. Weigh ~0.2 to 4 mg frozen arterial tissue in 1.7 mL micro-centrifuge tubes.
2. Using a 0.2 mL micro tissue grinder, homogenize tissue for 2 min on ice in 100–200 μL of 80% ethanol containing 0.4 nM 2-Cl-E$^+$-d_5.
3. Transfer the homogenate to a 1.7 mL micro-centrifuge tube and centrifuge for 20 min at 17,000 × g at 4 °C.
4. Transfer 50 μL of supernate to a HPLC vial with 250 μL glass insert and cap. Place samples in the LC–MS auto injector, and keep at 7 °C prior to 5 μL injection and analysis.

5.3.3.2. Preparation of 2-Cl-E$^+$ standards

1. In the dark prepare 0.5 nM 2-Cl-E$^+$ in 80% ethanol containing 0.4 nM 2-Cl-E$^+$-d_5.
2. Prepare a series of dilutions using the 0.5 nM 2-Cl-E$^+$ solution prepared in Step 1 to give 0.1, 0.2, 0.3 and 0.4 in 80% ethanol containing 0.4 nM 2-Cl-E$^+$-d_5.
3. Inject 5 μL standard to generate a standard curve. Standards should be prepared fresh for each experiment.

6. *Ex vivo* detection of 2-Cl-E$^+$ in arterial tissue

6.1. Materials

- Homogenization buffer. PBS (containing 0.05 M diethylenetriamine pentaacetic acid (DTPA), 1 × Roche cOmplete™ protease inhibitor; 11697498001). Can be stored at 4 °C for 2 weeks.
- 20 mM Trolox®. Dissolve 5 mg of Trolox® (Sigma-Aldrich; 238813) in 1 mL ethanol pre-flushed with N_2. Store at -20 °C for <6 months.
- 1 mM HE (prepared as described under Synthesis of 2-chloroethidium and 2-chloroethidium-d_5)
- Internal standard. Under dim lighting, dilute stock 2-Cl-E$^+$-d_5 to 3 μM in ethanol pre-flushed with N_2. Keep at 4 °C for <6 months.

- 20 mg/mL glucose. Dissolve 20 mg of glucose (Sigma-Aldrich; G7538) in 1 mL homogenization buffer.
- 40 μg/mL glucose oxidase. Dilute stock glucose oxidase (Sigma-Aldrich; G6891) to 241 μg/mL in homogenization buffer and filter through a Sephadex G-25 column (GE Healthcare; 17-0854-02). Dilute the glucose oxidase filtrate further to 40 μg/mL in homogenization buffer. Prepare fresh each time and use within 1 h.

6.2. Equipment

- 0.2 mL Micro tissue grinder (Wheaton; 357848)
- A microtube centrifuge (Thermo Scientific Heraeus Fresco 17 centrifuge)
- Sephadex G-25 column (GE Healthcare; 17-0854-02)
- 250 μL Glass inserts with polymer feet (Agilent, 5181-1270)
- PTFE/red silicone septa (Agilent, 5182-0731)
- Amber 2 mL screw top HPLC vials (Agilent, 5188-0716)
- Screw top lid for HPLC vials (Agilent, 5182-0728)

6.3. Instrumentation

- HPLC system (*e.g.*, Agilent 1290 UHPLC) connected to a triple-quadrupole mass spectrometer (*e.g.*, Agilent 6490 triple-quadrupole) or similar equipment capable of performing multiple reaction monitoring in positive ion mode.

6.4. Protocols

6.4.1. Homogenization of arterial tissue and treatment with HE/glucose/glucose oxidase

1. Weigh 0.2–5 mg frozen arterial tissue in 1.7 mL micro-centrifuge tubes.
2. Using a micro tissue grinder, homogenize tissue in 0.2 mL homogenization buffer for 2 min on ice.
3. Transfer the homogenate to a 1.7 mL micro-centrifuge tube, centrifuge for 3 min at 4000 × *g* at 4 °C, and remove supernate.
4. Determine the protein concentration of the supernate using the Bicinchoninic assay and bovine serum albumin (BSA) as a standard.
5. Transfer 80 μL supernate (~0.2 to 1.0 mg/mL) to a fresh 1.7 mL micro-centrifuge tube placed on ice and add 5 μL of each of the reagents listed below in the dark. Add the glucose oxidase last to initiate oxidation.
   - 20 mM Trolox®
   - 20 mg/mL glucose
   - 1 mM HE
   - 40 μg/mL glucose oxidase
6. Vortex for 5 s and incubate the mixture at 37 °C for 30 min in the dark. After incubation, centrifuge the reaction mixture at 17,000 × *g* for 1 min at 4 °C.
7. Add 5 μL internal standard (3 μM 2-Cl-E$^+$-d_5) to the mixture. Extract the HE oxidation products by adding 20 μL of mixture to 80 μL of ethanol pre-flushed with N_2 and leaving the extract on ice in the dark for 15 min.
8. Centrifuge extract at 17,000 × *g* for 20 min at 4 °C.
9. Transfer 50 μL of the resulting supernate to an HPLC vial with 250 μL glass insert and cap. Place samples in the LC–MS auto injector, and keep at 7 °C prior to injection and analysis.

6.4.2. Preparation of 2-Cl-E$^+$ standards

1. In the dark prepare 0.5 μM 2-Cl-E$^+$ in homogenization buffer.
2. Prepare a series of dilutions using 0.5 μM 2-Cl-E$^+$ to give 0.1, 0.2, 0.3, 0.4 and 0.5 μM standards.
3. Follow steps 10–13 listed under the subsection *Homogenization of arterial tissue and treatment with HE/glucose/glucose oxidase*.
4. Inject 2 μL of standard to generate a standard curve. Standards should be prepared fresh for each experiment.

7. LC–MS/MS analysis of *in vivo* and *ex vivo* of HE and oxidation products of HE

The conditions for LC–MS/MS analysis of 2-Cl-E$^+$ are shown in Table 2.

1. Connect the Synergi Polar-RP 4 μm column (250 × 2.1 mm) with guard to the HPLC and set the flow rate to 0.2 mL/min. Initially use 50% mobile phase A and 50% mobile phase B (see Table 2).
2. Use the gradient shown in Table 2 to separate 2-Cl-E$^+$ from HE and other HE oxidation products.
3. Use the parameters shown in Table 2 for MS gases, temperatures and voltages.
4. Detect 2-Cl-E$^+$, HE and the other HE oxidation products using the transitions and collision energy (CE) values shown in Table 3. *Note*: retention times for HE oxidation products can vary over time and/or between analyses.

8. Calculations and expected results

Fig. 4 shows representative chromatograms of 2-Cl-E$^+$ detected in atherosclerotic lesions at various anatomical sites from the mouse model of vulnerable atherosclerotic plaque [44], using the *in vivo* and ex *vivo* procedures, respectively. *In vivo* formation of 2-Cl-E$^+$ was detected in both stable and unstable atherosclerotic plaques of the right carotid artery, whereas it was absent in the corresponding lesion-free left carotid artery (Fig. 4A). Application of the *ex vivo* procedure resulted in the detection of 2-Cl-E$^+$ in stable and unstable atherosclerotic plaques of the right carotid artery, the aortic arch and aortic root (Fig. 4B), whereas 2-Cl-E$^+$ was not detected in the lesion-free left carotid artery.

Steps used to quantify the amounts of 2-Cl-E$^+$ formed *in vivo* and *ex vivo* are listed in Table 4. The concentration of 2-Cl-E$^+$ is determined by extrapolating the ratio of the m/z 348→318 (row 5) to m/z 353→318 transitions (row 6) from the standard curves of the 2-Cl-E$^+$:2-Cl-E$^+$-d_5 (row 7). The m/z 348→318 and m/z 353→

Table 2
Parameters for the detection of 2-Cl-E$^+$ and HE oxidation products by LC–MS.

Instrument	LC triple quadrupole mass spectrometer or similar instrument capable of MRM in the positive ion mode		
Mobile phase A	0.1% Formic acid in water		
Mobile phase B	0.1% Formic acid in acetonitrile		
Column	Synergi Polar-RP 4 μm, 250 × 2.1 mm		
Gradient	Time (min)	A (%)	B (%)
	0	50	50
	9	41	59
	17	35	65
	19	0	100
	21	50	50
	25	50	50
Flow rate	0.1 mL/min		
Typical inj. vol.	2 μL		
Capillary voltage	+4 kV		
Gas temperature	290 °C		
Sheath gas (N_2) flow	11 L/min		
Sheath gas (N_2) heater	350 °C		
Nebulizer pressure	20 p.s.i		
Scan range	50–1000 m/z		

Table 3
MRM transitions for HE and its oxidation products.

Compound	Transition (m/z)	CE (V)	~Retention time (min)
HE*	316.2→210.1	33	5.2
HE**	316.2→287.1	17	5.2
2-OH-E$^+$*	330.2→300.0	37	6.8
2-OH-E$^+$**	330.2→254.9	50	6.8
E$^+$*	314.2→285.1	25	8.1
E$^+$**	314.2→269.1	25	8.1
E$^+$-E$^+$ dimer*	313.2→299.1	17	11
E$^+$-E$^+$ dimer**	313.2→284.1	29	11
2-Cl-E$^+$*	348→318.1	35	10.3
2-Cl-E$^+$**	348→242.1	35	10.3
2-Cl-E$^+$-d_5*	353→318.1	41	10.3
2-Cl-E$^+$-d_5**	353→242.1	41	10.3

* and ** denote quantifier and qualifier transition, respectively.

Table 4
Example calculation for the amount of *in vivo* and *ex vivo* 2-Cl-E$^+$ measured.

	In vivo	*Ex vivo*
(1) Sample ID	Stable plaque	Stable plaque
(2) Weight (mg)	0.51	1.3
(3) Protein concentration in homogenate (mg/mL)		0.66
(4) Protein amount per injection μg/injection		0.211
(5) Peak Height 2-Cl-E$^+$ (348→318.1)	928	13,649
(6) Peak Height 2-Cl-E$^+$-d_5 (353→318.1)	2808	149
(7) 2-Cl-E$^+$/2-Cl-E$^+$-d_5	0.22 fmol	41.45 pmol
(8) 2-Cl-E$^+$/2-Cl-E$^+$-d_5	0.43 fmol/wet weight	196.3 pmol/mg protein

A homogenate prepared from stable plaque from the right carotid artery of a mouse model of vulnerable atherosclerotic plaque was extracted and subjected to LC–MS/MS analysis as described in Procedures using the 348→318.1 MRM transition.

318 transitions are characteristic for 2-Cl-E$^+$ and 2-Cl-E$^+$-d_5, respectively. To quantify the amounts of 2-Cl-E$^+$ formed *in vivo*, the 2-Cl-E$^+$ determined is normalized to wet weight of tissue (row 2), and expressed as fmol 2-Cl-E$^+$/2-Cl-E$^+$-d_5/wet weight (row 8). The amount of 2-Cl-E$^+$ detected *ex vivo* is normalized to the amount of protein contained in the sample injected (row 4) and is expressed as pmol 2-Cl-E$^+$/2-Cl-E$^+$-d_5/mg protein (row 8).

In addition to the detection of 2-Cl-E$^+$, formation of the HE oxidation products E$^+$, E$^+$-E$^+$ and 2-OH-E$^+$ can also be assessed. For example, Fig. 5 shows the LC–MS/MS chromatograms of *in vivo* 2-Cl-E$^+$, E$^+$, E$^+$-E$^+$ and 2-OH-E$^+$ detected in the "cuffed" artery from the mouse model of inflammation [38].

8.1. Caveats

Pitfalls in measuring HE oxidation products in biological systems have been described previously in detail [41,55]. Listed below are caveats relevant to the assessment of MPO activity by conversion of HE to 2-Cl-E$^+$.

8.1.1. Limits of detecting MPO activity

Enzymatically active MPO is present in human atherosclerotic lesions [15,56–58]. As a result, it is anticipated that active MPO may also be detected in murine atherosclerotic lesions. Indeed, our results from the *in vivo* formation of 2-Cl-E$^+$ suggest, for the first time, the presence of MPO activity in murine atherosclerotic lesions in the carotid artery of a model of vulnerable atherosclerotic plaque [44]. In this model of atherosclerosis, *in vivo* formation of 2-Cl-E$^+$ was not detected in the aortic root (Fig. 6), despite the presence of both E$^+$ and 2-OH-E$^+$. The latter observation indicates that the HE probe reached the target tissue and that $O_2^{\cdot -}$ (and hence likely also H_2O_2) were formed in atherosclerotic lesions at that arterial site. Moreover, the *ex vivo* procedure for MPO activity assessment revealed 2-Cl-E$^+$ formation in lesions from the aortic root and arch (Fig. 4B). In contrast, *in vivo* and *ex vivo* formation of 2-Cl-E$^+$ was not observed in lesion-free arterial segments, such as the left carotid artery (Fig. 4). Together, these findings suggest that in this model of vulnerable atherosclerotic plaque in mice, lesions at different anatomical sites contain variable amounts of MPO activity.

8.1.2. Competing substrates for HE

The yield of 2-Cl-E$^+$ generated is dependent on the tissue content of MPO and substrates competing for HE. HE reacts more effectively with $O_2^{\cdot -}$ ($2 \times 10^6\ M^{-1}\ s^{-1}$) [59] than HOCl

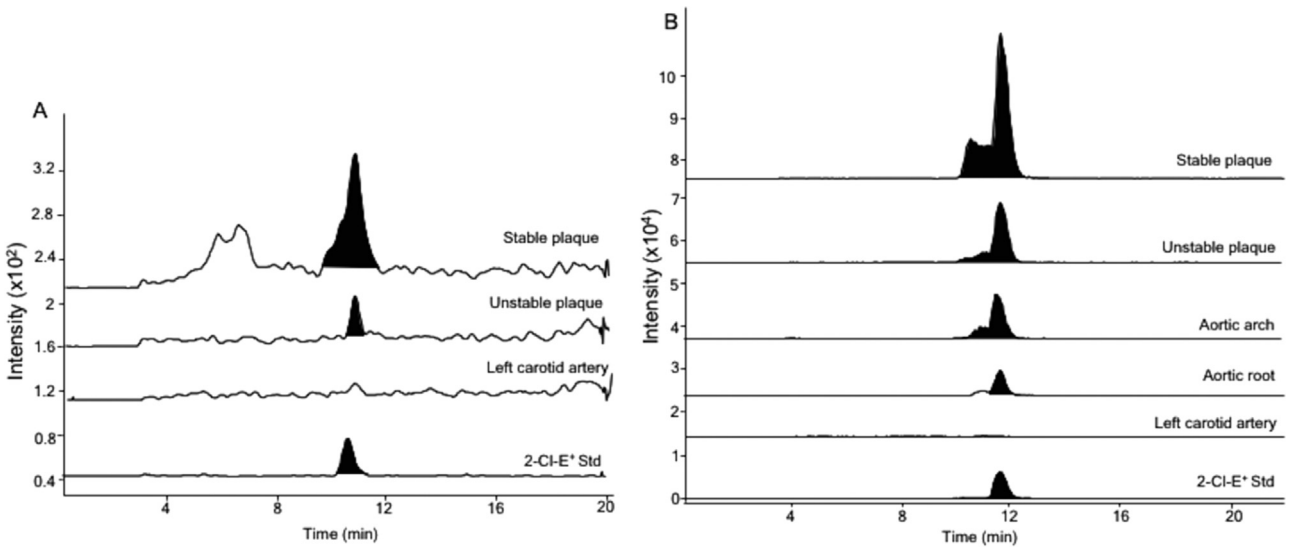

Fig. 4. Representative LC–MS/MS chromatograms of the m/z 348→318.1 transition of arterial tissue from a mouse model of vulnerable atherosclerotic plaque. Vulnerable atherosclerotic plaques were induced as described in the legend to Fig. 2. (A) *In vivo* formation of 2-Cl-E$^+$ was detected in stable and unstable plaques of the right carotid artery, but not in lesions at the aortic root and arch, or in the lesion-free left carotid artery. HE (80 μL of 20 mM) was administered by intravenous injection 7 weeks after tandem stenosis and 45 min prior to tissue collection. (B) *Ex vivo* 2-Cl-E$^+$ detected in stable and unstable plaques of the right carotid artery, and in lesions at the aortic root and arch, but absent in the lesion-free left carotid artery. For 2-Cl-E$^+$ *ex vivo* analysis, the homogenized arterial tissue was supplemented with 50 μM HE and glucose/glucose oxidase and then incubated for 30 min at 37 °C prior to extraction and LC–MS/MS analysis.

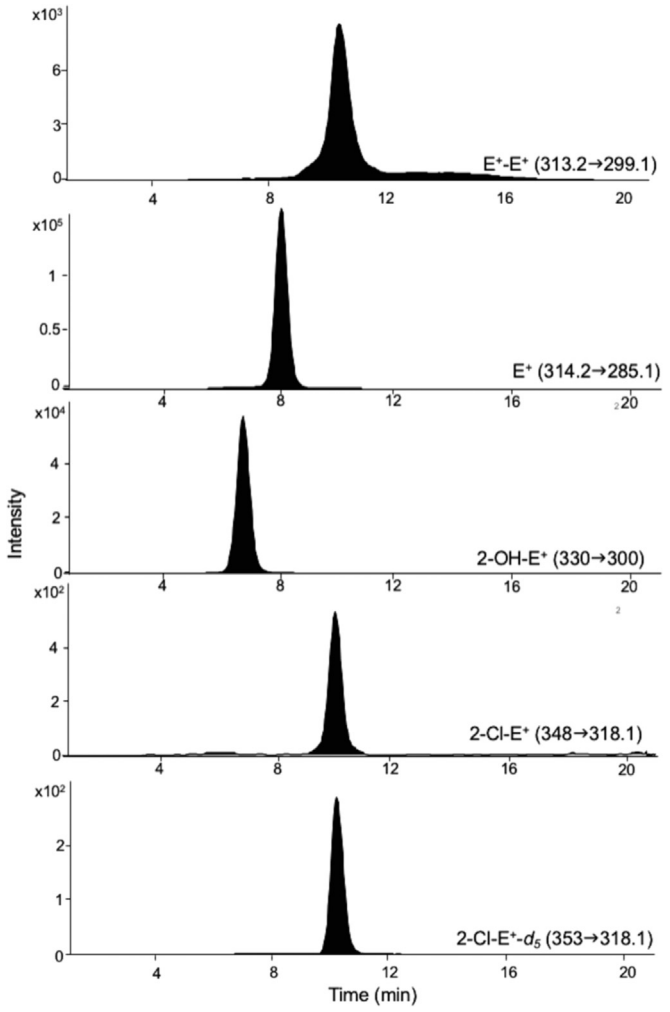

Fig. 5. Representative LC–MS/MS chromatograms of *in vivo* formed E^+-E^+, E^+ 2-OH-E^+, 2-Cl-E^+ and internal standard 2-Cl-E^+-d_5 detected in the left "cuffed" femoral artery from a mouse model of inflammation. Mice (8-9 weeks) were fed chow for 1 week prior to the placement of a non-occlusive cuff around the left femoral artery to induce arterial inflammation for 14 days before HE (80 μl of 20 mM) was administered by intravenous injection as described previously [38]. Arterial tissue was homogenized in ethanol containing 0.4 pM 2-Cl-E^+-d_5 prior to LC–MS/MS detection of *in vivo* 2-Cl-E^+.

$(1.5 \times 10^5\ M^{-1}\ s^{-1})$ [38]. HE can also react with other oxidants including H_2O_2, hydroxyl radicals and peroxynitrite, as well as heme-containing proteins including MPO, ferricytochrome *c*, horseradish peroxidase, myoglobin, hemoglobin and mitochondrial respiratory complex IV. Indeed, Figs. 5 and 6 show that HE oxidation products besides 2-Cl-E^+ can be detected in mouse arterial tissue of the two models studied here. *In vitro*, radical scavenging agents such as Trolox® can be used to limit competitive oxidation of HE by radical mechanisms [38], although it remains to be established whether this is also the case *in vivo*.

8.1.3. Competing substrates for HOCl

The primary endogenous competitor of HE for HOCl are sulfur-containing amino acids that react with HOCl with rate constants of $\sim 3 \times 10^7\ M^{-1}\ s^{-1}$ [26]. Other competing substrates for HOCl include α-amino groups in peptides and phospholipids (second order rate constants $\sim 10^4$ to $10^5\ M^{-1}\ s^{-1}$) [26,60,61] and the antioxidants ascorbate ($\sim 6 \times 10^6\ M^{-1}\ s^{-1}$) and urate ($2 \times 10^5\ M^{-1}\ s^{-1}$) [62,63]. Therefore, for the *ex vivo* MPO activity assessment, it is recommended to optimize concentrations of HE and/or glucose oxidase to maximize the reaction of HE with HOCl for the experimental system tested.

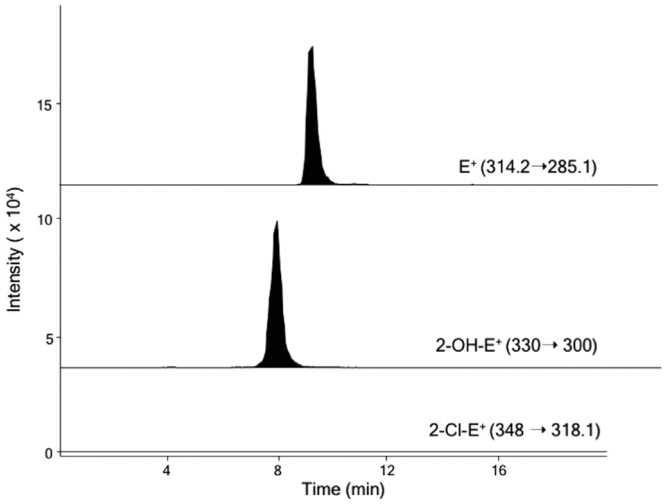

Fig. 6. Representative LC–MS/MS chromatograms of *in vivo* formed E^+ and 2-OH-E^+ (but not 2-Cl-E^+) in the aortic root from a mouse model of vulnerable atherosclerotic plaque. The experimental protocol used was identical to that described in the legend to Fig. 2.

8.1.4. Contaminating peaks

A critical issue we identified whilst developing the LC–MS/MS method was the presence of an unidentified analyte with a retention time 0.5 min earlier than that of 2-Cl-E^+, and that was extracted in the 348→318 MRM transition of 2-Cl-E^+. Specifically, the 348→318 and 348→242.1 Cl-E^+ MRM transitions acquired from the 'cuffed' left femoral artery of an *Apoe*$^{-/-}$ mouse from a model of arterial inflammation shows peaks eluting at accurate retention time (Fig. 7). In contrast, the inflamed left femoral artery from the same model except using a *Mpo*$^{-/-}$*Apoe*$^{-/-}$ mouse revealed a 348→318 MRM transition peak that eluted 0.5 min before authentic 2-Cl-E^+ standard, and had a height ~100-times smaller than 2-Cl-E^+ detected in the *Apoe*$^{-/-}$ mouse (Fig. 7). At first glance this analyte can easily be mistaken as 2-Cl-E^+, however, the absence of the 348 → 242.1 MRM transition and slightly different retention time confirm that this peak is not attributable to 2-Cl-E^+. To overcome this caveat it is essential to confirm the identity of 2-Cl-E^+ using the 348→242.1 MRM transition and to carefully compare the retention time with that of the 2-Cl-E^+-d_5 internal standard. We also found the degree of formation of this un-identified analyte differed between different suppliers of HE, with the Tyger HE (H12500) providing the lowest background for contaminating peaks and the best brand to use for 2-Cl-E^+ detection.

8.1.5. Photo-oxidation of HE

HE can undergo light-induced oxidation to form HE oxidation products, 2-OH-E^+ and E^+ [64]. Thus it is recommended to prepare HE mixtures and carry out all sample work-up procedures involving HE under dim lighting, away from fluorescent and artificial light.

8.1.6. Auto-oxidation of HE solutions

HE is susceptible to auto-oxidation when kept at room temperature for prolonged periods. Auto-oxidation can be minimized by adding DTPA, however, avoid adding high (> 50 μM) concentrations of DTPA, as DTPA-derived radicals can react with O_2 to form $O_2^{\cdot -}$ [59]. For longer-term storage, HE mixtures should be kept at −80 °C.

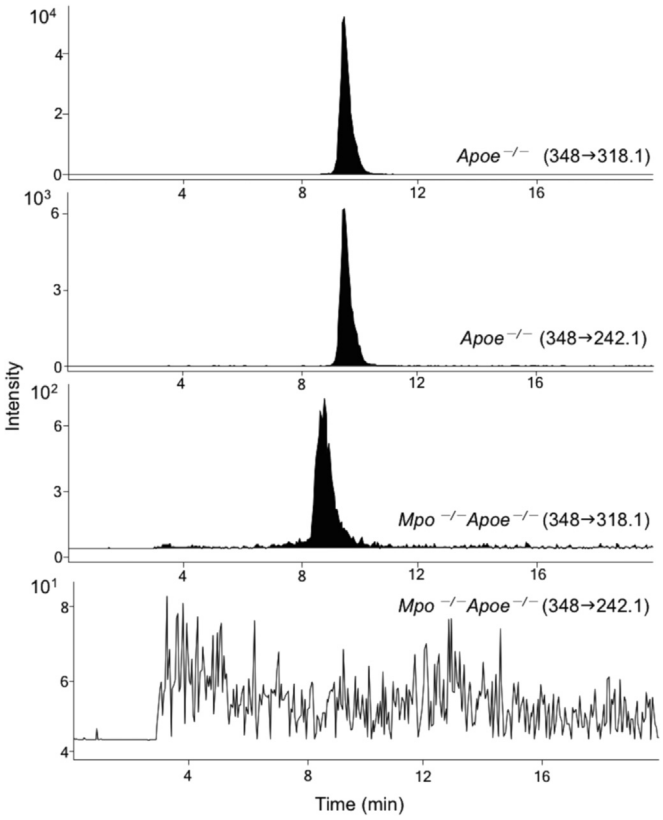

Fig. 7. Representative LC–MS/MS chromatograms of the 348→318.1 and 348→242.1 transitions acquired from the "cuffed" femoral artery of a male *Apoe*$^{-/-}$ and *Mpo*$^{-/-}$*Apoe*$^{-/-}$ mouse. Mice (8–9 weeks) were fed chow for 1 week prior to the placement of a non-occlusive cuff around the left femoral artery to induce arterial inflammation, with tissue collected 14 days after cuff placement as described [38]. 2-Cl-E^{+} *ex vivo* was detected in homogenized arterial tissue supplemented with 50 μM HE and glucose/glucose oxidase and then incubated for 30 min at 37 °C. The peak detected in arterial tissue from *Apoe*$^{-/-}$ *mice* is assigned to 2-Cl-E^{+} based on its retention time and presence of the 348→242.1 MRM transition. The peak detected in arterial tissue from *Mpo*$^{-/-}$*Apoe*$^{-/-}$ mice using the 348→318.1 transition is ~100-fold smaller in height than the corresponding peak in arterial tissue from *Apoe*$^{-/-}$ mice, and it cannot be assigned to 2-Cl-E^{+} because the 348→242.1 transition is absent, and its retention time 0.5 min earlier than that authentic 2-Cl-E^{+} standard.

Acknowledgements

We thank Darren Newington for technical assistance in animal surgery. We also thank the Victor Chang Cardiac Research Institute for infrastructure support.

References

[1] S.J. Nicholls, S.L. Hazen, Myeloperoxidase and cardiovascular disease, Arterioscler. Thromb. Vasc. Biol. 25 (2005) 1102–1111.
[2] R.K. Schindhelm, L.P. van der Zwan, T. Teerlink, P.G. Scheffer, Myeloperoxidase: a useful biomarker for cardiovascular disease risk stratification? Clin. Chem. 55 (8) (2009) 1462–1470.
[3] M.J. Davies, C.L. Hawkins, D.I. Pattison, M.D. Rees, Mammalian heme peroxidases: from molecular mechanisms to health implications, Antioxd. Redox Signal. 10 (2008) 1199–1234.
[4] C.C. Winterbourn, A.J. Kettle, Redox reactions and microbial killing in the neutrophil phagosome, Antioxid. Redox Signal. 18 (2013) 642–660.
[5] A. Daugherty, J.L. Dunn, D.L. Rateri, J.W. Heinecke, Myeloperoxidase, a catalyst for lipoprotein oxidation, is expressed in human atherosclerotic lesions, J. Clin. Invest. 94 (1994) 437–444.
[6] J.P. Eiserich, S. Baldus, M.L. Brennan, W. Ma, C. Zhang, A. Tousson, L. Castro, A. J. Lusis, W.M. Nauseef, C.R. White, B.A. Freeman, Myeloperoxidase, a leukocyte-derived vascular NO oxidase, Science 296 (2002) 2391–2394.
[7] R. Stocker, A. Huang, E. Jeranian, J.Y. Hou, T. Wu, S.R. Thomas, J.F. Keaney Jr., Hypochlorous acid impairs EDNO bioactivity through a superoxide-dependent mechanism, Arterioscler. Thromb. Vasc. Biol. 24 (2004) 2028–2033.
[8] J.A. Vita, M.L. Brennan, N. Gokce, S.A. Mann, M. Goormastic, M.H. Shishehbor, M.S. Penn, J.F. Keaney Jr., S.L. Hazen, Serum myeloperoxidase levels independently predict endothelial dysfunction in humans, Circulation 110 (2004) 1134–1139.
[9] S. Baldus, C. Heeschen, T. Meinertz, A.M. Zeiher, J.P. Eiserich, T. Münzel, M. L. Simoons, C.W. Hamm, Myeloperoxidase serum levels predict risk in patients with acute coronary syndromes, Circulation 108 (2003) 1440–1445.
[10] M.L. Brennan, M.S. Penn, F. Van Lente, V. Nambi, M.H. Shishehbor, R.J. Aviles, M. Goormastic, M.L. Pepoy, E.S. McErlean, E.J. Topol, S.E. Nissen, S.L. Hazen, Prognostic value of myeloperoxidase in patients with chest pain, N. Engl. J. Med. 349 (2003) 1595–1604.
[11] B. Shao, M.N. Oda, J.F. Oram, J.W. Heinecke, Myeloperoxidase: an oxidative pathway for generating dysfunctional high-density lipoprotein, Chem. Res. Toxicol. 23 (2010) 447–454.
[12] E.A. Fisher, J.E. Feig, B. Hewing, S.L. Hazen, J.D. Smith, High-density lipoprotein function, dysfunction, and reverse cholesterol transport, Arterioscler. Thromb. Vasc. Biol. 32 (2012) 2813–2820.
[13] C. Weber, H. Noels, Atherosclerosis: current pathogenesis and therapeutic options, Nat. Med. 17 (2011) 1410–1422.
[14] R. Stocker, J.F. Keaney Jr., Role of oxidative modifications in atherosclerosis, Physiol. Rev. 84 (2004) 1381–1478.
[15] L.J. Hazell, L. Arnold, D. Flowers, G. Waeg, E. Malle, R. Stocker, Presence of hypochlorite-modified proteins in human atherosclerotic lesions, J. Clin. Invest. 97 (1996) 1535–1544.
[16] S.L. Hazen, J.W. Heinecke, 3-Chlorotyrosine, a specific marker of myeloperoxidase-catalyzed oxidation, is markedly elevated in low density lipoprotein isolated from human atherosclerotic intima, J. Clin. Invest. 99 (1997) 2075–2081.
[17] C. Bergt, S. Pennathur, X. Fu, J. Byun, K. O'Brien, T.O. McDonald, P. Singh, G. M. Anantharamaiah, A. Chait, J. Brunzell, R.L. Geary, J.F. Oram, J.W. Heinecke, The myeloperoxidase product hypochlorous acid oxidizes HDL in the human artery wall and impairs ABCA1-dependent cholesterol transport, Proc. Natl. Acad. Sci. USA 101 (2004) 13032–13037.
[18] A.K. Tiden, T. Sjogren, M. Svensson, A. Bernlind, R. Senthilmohan, F. Auchere, H. Norman, P.O. Markgren, S. Gustavsson, S. Schmidt, S. Lundquist, L.V. Forbes, N.J. Magon, L.N. Paton, G.N. Jameson, H. Eriksson, A.J. Kettle, 2-Thioxanthines are mechanism-based inactivators of myeloperoxidase that block oxidative stress during inflammation, J. Biol. Chem. 286 (2011) 37578–37589.
[19] K.F. Geoghegan, A.H. Varghese, X. Feng, A.J. Bessire, J.J. Conboy, R.B. Ruggeri, K. Ahn, S.N. Spath, S.V. Filippov, S.J. Conrad, P.A. Carpino, C.R. Guimaraes, F. F. Vajdos, Deconstruction of activity-dependent covalent modification of heme in human neutrophil myeloperoxidase by multistage mass spectrometry (MS (4)), Biochemistry 51 (2012) 2065–2077.
[20] P.G. Rausch, T.G. Moore, Granule enzymes of polymorphonuclear neutrophils: a phylogenetic comparison, Blood 46 (1975) 913–919.
[21] M.L. Brennan, M.M. Anderson, D.M. Shih, X.D. Qu, X. Wang, A.C. Mehta, L. L. Lim, W. Shi, S.L. Hazen, J.S. Jacob, J.R. Crowley, J.W. Heinecke, A.J. Lusis, Increased atherosclerosis in myeloperoxidase-deficient mice, J. Clin. Invest. 107 (2001) 419–430.
[22] T.S. McMillen, J.W. Heinecke, R.C. LeBoeuf, Expression of human myeloperoxidase by macrophages promotes atherosclerosis in mice, Circulation 111 (2005) 2798–2804.
[23] L.W. Castellani, J.J. Chang, X. Wang, A.J. Lusis, W.F. Reynolds, Transgenic mice express human MPO −463G/A alleles at atherosclerotic lesions, developing hyperlipidemia and obesity in −463G males, J. Lipid Res. 47 (2006) 1366–1377.
[24] P.E. Morgan, R.P. Laura, R.A. Maki, W.F. Reynolds, M.J. Davies, Thiocyanate supplementation decreases atherosclerotic plaque in mice expressing human myeloperoxidase, Free Radic. Res. 49 (2015) 743–749.
[25] A.J. Kettle, A.M. Albrett, A.L. Chapman, N. Dickerhof, L.V. Forbes, I. Khalilova, R. Turner, Measuring chlorine bleach in biology and medicine, Biochim. Biophys. Acta 1840 (2) (2014) 781–793.
[26] D.I. Pattison, M.J. Davies, Absolute rate constants for the reaction of hypochlorous acid with protein side chains and peptide bonds, Chem. Res. Toxicol. 14 (2001) 1453–1464.
[27] S. Fu, H. Wang, M.J. Davies, R. Dean, Reactions of hypochlorous acid with tyrosine and peptidyl-tyrosyl residues give dichlorinated and aldehydic products in addition to 3-chlorotyrosine, J. Biol. Chem. 275 (2000) 10851–10858.
[28] A.R. Mani, S. Ippolito, J.C. Moreno, T.J. Visser, K.P. Moore, The metabolism and dechlorination of chlorotyrosine in vivo, J. Biol. Chem. 282 (2007) 29114–29121.
[29] T. Franck, S. Kohnen, K.Z. Boudjeltia, P. Van Antwerpen, A. Bosseloir, A. Niesten, O. Gach, M. Nys, G. Deby-Dupont, D. Serteyn, A new easy method for specific measurement of active myeloperoxidase in human biological fluids and tissue extracts, Talanta 80 (2009) 723–729.
[30] A.L. Chapman, T.J. Mocatta, S. Shiva, A. Seidel, B. Chen, I. Khalilova, M.E. Paumann-Page, G.N. Jameson, C.C. Winterbourn, A.J. Kettle, Ceruloplasmin is an endogenous inhibitor of myeloperoxidase, J. Biol. Chem. 288 (2013) 6465–6477.
[31] B. Pulli, M. Ali, R. Forghani, S. Schob, K.L. Hsieh, G. Wojtkiewicz, J.J. Linnoila, J. W. Chen, Measuring myeloperoxidase activity in biological samples, PLoS One 8 (2013) e67976.
[32] T. Franck, G. Minguet, C. Delporte, S. Derochette, K. Zouaoui Boudjeltia, P. Van Antwerpen, O. Gach, G. Deby-Dupont, A. Mouithys-Mickalad, D. Serteyn, An immunological method to combine the measurement of active and total myeloperoxidase on the same biological fluid, and its application in finding inhibitors which interact directly with the enzyme, Free Radic. Res. 49 (2015)

790–799.
[33] R.J. Goiffon, S.C. Martinez, D. Piwnica-Worms, A rapid bioluminescence assay for measuring myeloperoxidase activity in human plasma, Nat. Commun. 6 (2015) 6271.
[34] A.A. Kapralov, I.V. Kurnikov, Vlasova II, N.A. Belikova, V.A. Tyurin, L.V. Basova, Q. Zhao, Y.Y. Tyurina, J. Jiang, H. Bayir, Y.A. Vladimirov, V.E. Kagan, The hierarchy of structural transitions induced in cytochrome c by anionic phospholipids determines its peroxidase activation and selective peroxidation during apoptosis in cells, Biochemistry 46 (2007) 14232–14244.
[35] J. Zielonka, J.D. Lambeth, B. Kalyanaraman, On the use of L-012, a luminol-based chemiluminescent probe, for detecting superoxide and identifying inhibitors of NADPH oxidase: a reevaluation, Free Radic. Biol. Med. 65 (2013) 1310–1314.
[36] A.K. Thukkani, J. McHowat, F.F. Hsu, M.L. Brennan, S.L. Hazen, D.A. Ford, Identification of alpha-chloro fatty aldehydes and unsaturated lysophosphatidylcholine molecular species in human atherosclerotic lesions, Circulation 108 (2003) 3128–3133.
[37] A. van der Vliet, J.P. Eiserich, B. Halliwell, C.E. Cross, Formation of reactive nitrogen species during peroxidase-catalyzed oxidation of nitrite. A potential additional mechanism of nitric oxide-dependent toxicity, J. Biol. Chem. 272 (1997) 7617–7625.
[38] G.J. Maghzal, K.M. Cergol, S.R. Shengule, C. Suarna, D. Newington, A.J. Kettle, R. J. Payne, S. R., Assessment of myeloperoxidase activity by the conversion of hydroethidine to 2-chloroethidium, J. Biol. Chem. 259 (2014) 5580–5595.
[39] G. Rothe, G. Valet, Flow cytometric analysis of respiratory burst activity in phagocytes with hydroethidine and 2′,7′-dichlorofluorescin, J. Leukoc. Biol. 47 (1990) 440–448.
[40] H. Zhao, J. Joseph, H.M. Fales, E.A. Sokoloski, R.L. Levine, J. Vasquez-Vivar, B. Kalyanaraman, Detection and characterization of the product of hydroethidine and intracellular superoxide by HPLC and limitations of fluorescence, Proc. Natl. Acad. Sci. USA 102 (2005) 5727–5732.
[41] J. Zielonka, S. Srinivasan, M. Hardy, O. Ouari, M. Lopez, J. Vasquez-Vivar, N. G. Avadhani, B. Kalyanaraman, Cytochrome c-mediated oxidation of hydroethidine and mito-hydroethidine in mitochondria: identification of homo- and heterodimers, Free Radic. Biol. Med. 44 (2008) 835–846.
[42] J. Zielonka, B. Kalyanaraman, Hydroethidine- and MitoSOX-derived red fluorescence is not a reliable indicator of intracellular superoxide formation: Another inconvenient truth, Free Radic. Biol. Med. 48 (2010) 983–1001.
[43] M. Moroi, L. Zhang, T. Yasuda, R. Virmani, H.K. Gold, M.C. Fishman, P.L. Huang, Interaction of genetic deficiency of endothelial nitric oxide, gender, and pregnancy in vascular response to injury in mice, J. Clin. Invest. 101 (1998) 1225–1232.
[44] Y.C. Chen, A.V. Bui, J. Diesch, R. Manasseh, C. Hausding, J. Rivera, I. Haviv, A. Agrotis, N.M. Htun, J. Jowett, C.E. Hagemeyer, R.D. Hannan, A. Bobik, K. Peter, A novel mouse model of atherosclerotic plaque instability for drug testing and mechanistic/therapeutic discoveries using gene and microRNA expression profiling, Circ. Res. 113 (2013) 252–265.
[45] A.V. Biziukin, L.G. Korkina, B.T. Velichkovskii, [Comparative use of 2,7-dichlorofluorescein diacetate, dihydrorhodamine 123, and hydroethidine for studying oxidative metabolism of phagocytosing cells], Biull. Eksp. Biol. Med. 119 (1995) 361–365.
[46] A.J. Kettle, Neutrophils convert tyrosyl residues in albumin to chlorotyrosine, FEBS Lett. 379 (1996) 103–106.
[47] S. Fu, H. Wang, M. Davies, R. Dean, Reactions of hypochlorous acid with tyrosine and peptidyl-tyrosyl residues give dichlorinated and aldehydic products in addition to 3- chlorotyrosine, J. Biol. Chem. 275 (2000) 10851–10858.
[48] M.M. Kockx, G.R. De Meyer, L.J. Andries, H. Bult, W.A. Jacob, A.G. Herman, The endothelium during cuff-induced neointima formation in the rabbit carotid artery, Arterioscler. Thromb. Vasc. Biol. 13 (1993) 1874–1884.
[49] D.J. Van Put, N. Van Osselaer, G.R. De Meyer, L.J. Andries, M.M. Kockx, L.S. De Clerck, H. Bult, Role of polymorphonuclear leukocytes in collar-induced intimal thickening in the rabbit carotid artery, Arterioscler. Thromb. Vasc. Biol. 18 (1998) 915–921.
[50] J.L. Vivero-Escoto, I.I. Slowing, V.S. Lin, Tuning the cellular uptake and cytotoxicity properties of oligonucleotide intercalator-functionalized mesoporous silica nanoparticles with human cervical cancer cells HeLa, Biomaterials 6 (2010) 1325–1333.
[51] S.A. Ross, M. Pitie, B. Meunier, A straightforward preparation of primary alkyl triflates and their utility in the synthesis of derivatives of ethidium, J. Chem. Soc. Perkin Trans. 1 (2000) (2000) 571–574.
[52] K. Kundu, S.F. Knight, S. Lee, W.R. Taylor, N. Murthy, A significant improvement of the efficacy of radical oxidant probes by the kinetic isotope effect, Angew. Chem. Int. Ed. Engl. 49 (2010) 6134–6138.
[53] J. Zielonka, H. Zhao, Y. Xu, B. Kalyanaraman, Mechanistic similarities between oxidation of hydroethidine by Fremy's salt and superoxide: stopped-flow optical and EPR studies, Free Radic. Biol. Med. 39 (2005) 853–863.
[54] T. Yardeni, M. Eckhaus, H.D. Morris, M. Huizing, S. Hoogstraten-Miller, Retro-orbital injections in mice, Lab. Anim. 40 (2011) 155–160.
[55] J. Zielonka, M. Hardy, B. Kalyanaraman, HPLC study of oxidation products of hydroethidine in chemical and biological systems: ramifications in superoxide measurements, Free Radic. Biol. Med. 46 (2009) 329–338.
[56] L.J. Hazell, G. Baernthaler, R. Stocker, Correlation between intima-to-media ratio, apolipoprotein B-100, myeloperoxidase and hypochlorite-oxidized proteins in human atherosclerosis, Free Radic. Biol. Med. 31 (2001) 1254–1262.
[57] S.L. Hazen, J.R. Crowley, D.M. Mueller, J.W. Heinecke, Mass spectrometric quantification of 3-chlorotyrosine in human tissues with attomole sensitivity: a sensitive and specific marker for myeloperoxidase-catalyzed chlorination at sites of inflammation, Free. Radic. Biol. Med. 23 (1997) 909–916.
[58] E. Malle, G. Waeg, R. Schreiber, E.F. Grone, W. Sattler, H.J. Grone, Immunohistochemical evidence for the myeloperoxidase/H_2O_2/halide system in human atherosclerotic lesions: colocalization of myeloperoxidase and hypochlorite-modified proteins, Eur. J. Biochem. 267 (2000) 4495–4503.
[59] J. Zielonka, T. Sarna, J.E. Roberts, J.F. Wishart, B. Kalyanaraman, Pulse radiolysis and steady-state analyses of the reaction between hydroethidine and superoxide and other oxidants, Arch. Biochem. Biophys. 456 (2006) 39–47.
[60] J.M. Antelo, F. Arce, M. Parajó, Kinetic study of the formation of N-chloramines, Int. J. Chem. Kinet. 27 (1995) 637–647.
[61] P. Nagy, M.T. Ashby, Kinetics and mechanism of the oxidation of the glutathione dimer by hypochlorous acid and catalytic reduction of the chloroamine product by glutathione reductase, Chem. Res. Toxicol. 20 (2007) 79–87.
[62] C.C. Winterbourn, Comparative reactivities of various biological compounds with myeloperoxidase-hydrogen peroxide-chloride, and similarity of the oxidant to hypochlorite, Biochim. Biophys. Acta 840 (1985) 204–210.
[63] L.K. Folkes, L.P. Candeias, P. Wardman, Kinetics and mechanisms of hypochlorous acid reactions, Arch. Biochem. Biophys. 323 (1995) 120–126.
[64] J. Zielonka, J. Vasquez-Vivar, B. Kalyanaraman, The confounding effects of light, sonication, and Mn(III)TBAP on quantitation of superoxide using hydroethidine, Free Radic. Biol. Med. 41 (2006) 1050–1057.